J|A|C|S COMMUNICATIONS

Published on Web 09/16/2009

Cell-Targeted Self-Assembled DNA Nanostructures

Alexey Y. Koyfman,[†,§] Gary B. Braun,[‡] and Norbert O. Reich*[,†,‡]

Biomolecular Science and Engineering Program and Department of Chemistry and Biochemistry, University of California—Santa Barbara, Santa Barbara, California 93106-9510

Received February 28, 2009; E-mail: reich@chem.ucsb.edu

The ability to organize materials is a core goal of bionanotechnology. Biomedically relevant examples include the organization of cells into predictable architectures on surfaces[1,2] and the delivery of diverse molecules to cells.[3] Cell surface engineering[4] seeks to localize nanoscale materials such as proteins,[5] carbon nanotubes,[6] synthetic bioactive polymers,[7] vault nanoparticles,[8] and polyelectrolyte multilayer patches[9] onto cellular membranes. Cells have been assembled into microtissues using DNA-mediated interactions.[10] DNA scaffolds, which are nanoarrays built from repeating DNA motifs, have been used for multicomponent interactions[11] to position small peptides,[12] streptavidin,[13,14] antibodies,[15,16] and inorganic materials[17,18] on the array surface into controlled networks and to detect proteins,[19,20] DNA,[21] and RNA.[22] We demonstrate how self-assembled DNA arrays can be directed to the surface of cells, first through biotin−streptavidin interactions and second through specific antibody−cell surface interactions. The versatile cargo-carrying ability of arrays for directing cell-surface interactions, cell−cell bridging, and positioning multiple cells onto a DNA fabric is explored.

DNA nanoarrays provide a number of strategies to specifically label cell surfaces with functionalized micrometer-sized patches, deliver materials to cell surfaces, and engineer cell/cell networks. The porous and periodic nature of the DNA material could be useful for tissue engineering. Functionalized nanoarrays could be used for cancer cells screening, control of stem cell fate, and controlled activation of immune response.

We present two strategies for attaching hexagonal DNA arrays to human cells. First, biotin-modified arrays were bound to biotinylated cancer cells using streptavidin (STV) as a bridging component. Second, biotin-modified arrays attached to antibodies were bound to native epidermal growth factor receptors (EGFRs) expressed on certain cancer cells using STV and antibodies as bridging components. Arrays were assembled from three ssDNA strands (Figure 1a) into hexagonal units repeated every 30 nm (Figure 1b,c) and into extended networks spanning several micrometers (Figure 1d).[23−26] DNA arrays were visualized using the fluorescent nucleotide labeling system ULYSIS Alexa Fluor 488 (Figure 2b). An STV HiLyte Fluor 555 (STV-555) conjugate was immobilized on top of the three-point-star motifs in the arrays through the biotin on the middle thymine in the first T3 repeat of the 72 nucleotide long strand localized in the center of the star junction (Figure 1a). This resulted in a minimum separation of 17.5 nm between STVs (Figure 2a). Fluorescence from the covalently bound Alexa Fluor 488 colocalized with STV-555 fluorescence (Figure 2b,c). Further verification that STV was bound at high density onto the biotinylated DNA arrays was obtained using atomic force microscopy (AFM) (Figure 2d). Although a biotin was present on every three-point-star motif (Figure 1b), STV molecules were detected on only a subset of these (Figure 2d) because some biotins were inaccessible to the STVs. We further note that a DNA bilayer[25,26] containing STV molecules was observed (Figure 2d), possibly because the flexible array folded over onto itself and was bridged by STV.

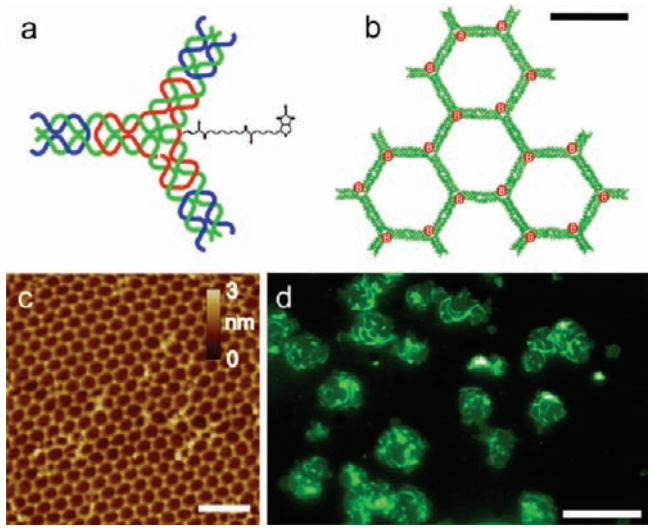

Figure 1. Assembly of fluorescent DNA hexagonal arrays. (a) Diagram of the biotinylated three-point-star monomer used to form the DNA arrays. (b) Diagram of an 18 unit biotinylated hexagonal DNA array (30 nm scale bar). (c) AFM image of a biotinylated hexagonal DNA array (100 nm scale bar). (d) Biotinylated hexagonal DNA arrays labeled with YOYO 1 on a mica surface (10 μm scale bar).

The first strategy for attaching DNA arrays to cells involves a nonspecific route using lysine-reactive biotin. Here, primary amines of membrane-bound proteins on the surface of Jurkat cells were reacted with membrane-impermeable NHS-biotin. The coverage of biotins on the Jurkat cell surface was confirmed by mixing biotinylated cells with STV-555 followed by observation using epifluorescent and confocal microscopy [Figures S1 and S2 in the Supporting Information (SI)]. Many STV-555 molecules were bound to the outside of biotinylated Jurkat cells, as observed using 565 nm (orange) fluorescence (Figure 3a). The treatment of biotinylated Jurkat cells with STV-modified DNA arrays (Figure 3b−e) resulted in larger numbers of arrays bound to biotinylated cells than the alternative scheme in which biotinylated cells incubated with STV were subsequently combined with biotinylated arrays (Figure 3a). Cells in the confocal images throughout this work were additionally labeled with cytosolic and plasma membrane dyes, pseudocolored blue and red respectively. DNA arrays fluoresce at 519 nm (green) (Figure 3b) (see Methods in the SI). Since the DNA arrays and cells were maintained at similar concentrations (10^6−10^7 per mL), we expected to have roughly one

[†] Biomolecular Science and Engineering Program.
[‡] Department of Chemistry and Biochemistry.
[§] Present address: National Center for Macromolecular Imaging, Verna and Marrs McLean Department of Biochemistry and Molecular Biology, Baylor College of Medicine, One Baylor Plaza, Houston, Texas 77030.

10.1021/ja9015638 CCC: $40.75

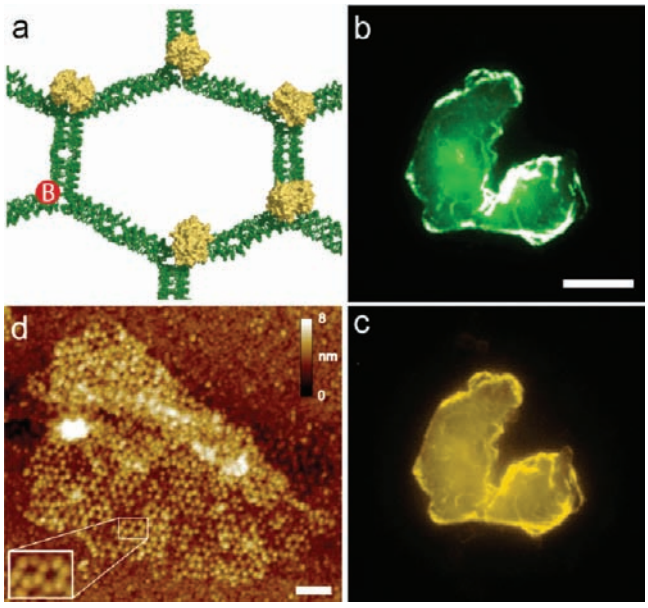

Figure 2. Attachment of STV to fluorescent DNA hexagonal arrays. (a) Diagram of a biotinylated hexagonal DNA array bound with STV. (b) Alexa Fluor 488 fluorescence of a DNA array attached to STVs (5 μm scale bar). (c) Fluorescence of STV-555 bound with a DNA array (5 μm scale bar). (d) AFM image of a biotinylated DNA array bound with STV (100 nm scale bar).

array bound per cell (Figure 3a,c). By superposing fluorescence and differential interference contrast (DIC) microscopy-based images, we observed examples of one or two arrays bound to a single cell (Figure 3c,d), an array bridging two cells (Figure 3e), and free arrays (Figure 3b). The existence of free arrays (17.9% of the total array count) and unbound cells was most likely due to incomplete mixing, excess cells, or excess STV. Free STV may interfere by passivating some cells against binding, thereby decreasing the efficiency of binding arrays to cells. Also, aggregation of arrays may occur during partial STV coating.

Our second strategy for directing DNA arrays to cancer cells builds on the previous strategy but uses interactions between cell-specific surface proteins and their antibodies. This approach provides a basis for directing the assembly of distinct cell types through the use of various cell-specific surface markers. EGFRs are overexpressed on the surface of many human cancer cells, at levels of up to 10^6 per cell.[27,28] Here we used two EGFR-expressing cell lines (HEK 293T and HeLa) and one nonexpressing control cell line (Jurkat)[28] along with a mouse EGFR antibody (Ab) with a biotin coupled within the constant region, enabling attachment to STV−DNA arrays. EGFR expression was confirmed with mouse anti-EFGR Ab's (528 IgG)[29] and a secondary goat anti-mouse Ab labeled with Alexa Fluor 488 (Figures S3−S5 in the SI).

Ab's were first added to STV arrays and then combined with (nonbiotinylated) cells by mixing for 1−2 h at room temperature at 50−100 rpm. Figure 4a shows a field view of HEK 293T cells attached to DNA arrays through the EGFR Ab. Again we observed both one and two arrays bound per cell as well as a single array bridging two cells (Figure 4c−f). Scanning electron microscopy (SEM) also showed attachment of DNA structures to HEK 293T cells (Figure 4b and Figure S6 in the SI). Jurkat cells lacking EGFRs did not attach to Ab DNA arrays (Figure S7 in the SI). Also, arrays not treated with the Ab did not bind to HEK 293T cells (Figure S8 in the SI).

DNA arrays bound to Ab's also attach to HeLa cells containing EGFRs (Figure 5). A field-view confocal microscopy image shows

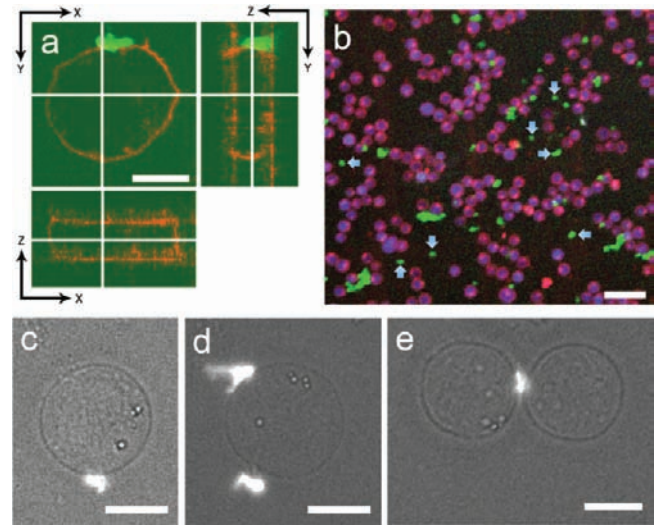

Figure 3. Attachment of fluorescent DNA hexagonal arrays through STV to biotinylated Jurkat cells. (a) Confocal microscopy cross section of a fluorescently labeled DNA−biotin−STV array bound to a biotinylated Jurkat cell. The DNA array is green, and the Jurkat cell surface is orange because of STV-555 (10 μm scale bar). (b) Confocal microscopy field view of fluorescently labeled DNA−biotin−STV arrays bound to biotinylated Jurkat cells. Unbound arrays are shown by light-blue arrows. DNA arrays are green and Jurkat cell surfaces red; Jurkat cytoplasm is blue (50 μm scale bar). For biotinylated Jurkat cells, 82.1% of the STV−DNA arrays were bound (N = 307), whereas only 12.5% of the arrays were bound when the cells were not biotinylated (N = 297). (c−e) Fluorescence micrographs of DNA−biotin−STV arrays bound to Jurkat−biotin cells. Cells are visualized in DIC mode (10 μm scale bar).

numerous arrays attached to HeLa cells (Figure 5a). Again, partial STV coating may have caused aggregate formation (Figure 5a). Presumably the bulky size of the aggregates impairs diffusion, hindering their binding to the cell surfaces. With excess EGFR Ab's, both arrays and cells contained Ab's, and therefore, the binding efficiency was further decreased by passivation. An excess of cells over arrays may cause a lower percentage of cells to bind to arrays (Figure 4a). We observed multiple small arrays bound to a cell

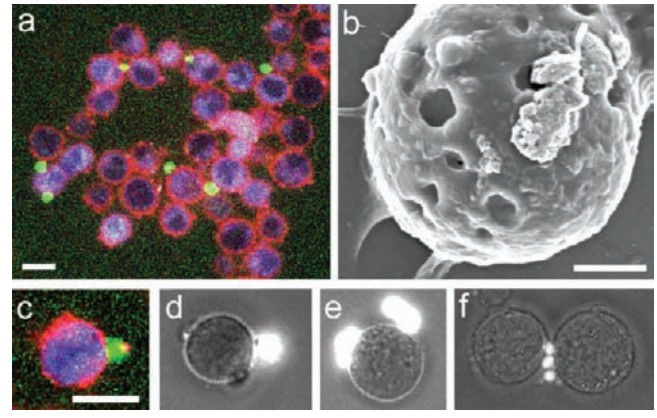

Figure 4. Attachment of fluorescent Ab−DNA hexagonal arrays to EGFRs of HEK 293T cells. (a, c) Confocal microscopy of fluorescently labeled DNA−biotin−STV−Ab arrays bound to EGFRs of HEK 293T cells through AB's. DNA arrays are green and HEK 293T cell surfaces red; HEK 293T cytoplasm is blue. (b) SEM image of a DNA−biotin−STV−Ab array bound to a HEK 293T cell through Ab's (2 μm scale bar). (d−f) Fluorescent DNA−biotin−STV−Ab arrays bound to EGFRs of HEK 293T cells through Ab's. Cells are visualized in DIC mode. The scale bars in (a) and (c−f) are 10 μm. Inclusion of the EGFR Ab's resulted in binding of 82.9% of the STV−DNA arrays (N = 292), whereas only 10.1% of the arrays were bound when the EGFR Ab was not present (N = 941).

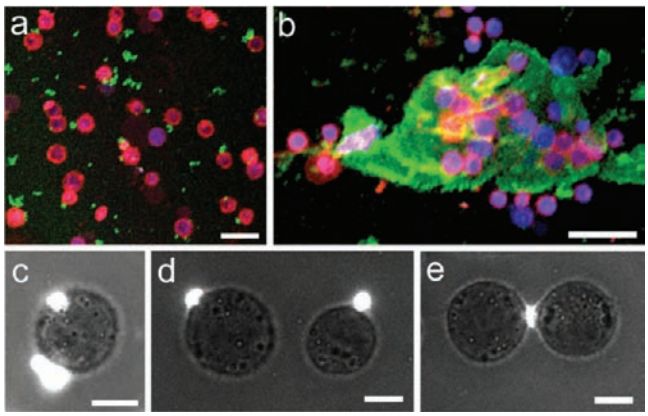

Figure 5. Attachment of fluorescent DNA hexagonal arrays to EGFRs of HeLa cells. (a) Confocal microscopy field view of DNA−biotin−STV−Ab arrays bound to EGFRs of HeLa cells through Ab's. DNA arrays are green and HeLa cell surfaces red; HeLa cytoplasm is blue (50 μm scale bar). (b) Confocal microscopy of a large DNA−biotin−STV−Ab array bound to EGFRs on multiple HeLa cells. DNA arrays are green and HeLa cell surfaces red; HeLa cytoplasm is blue (50 μm scale bar). In the presence of the EGFR Ab, 72.3% of the Ab−DNA arrays were bound to HeLa cells ($N = 328$), whereas 19.6% arrays were bound to cells in the absence of Ab ($N = 321$). (c−e) Fluorescent DNA−biotin−STV−Ab arrays bound to EGFRs of HeLa cells through Ab's, visualized in DIC mode (10 μm scale bar).

and larger arrays bridging many cells, as with the two previous cell lines (Figure 5a−e, Figure S10 in the SI). Binding of DNA−biotin−STV arrays to EGFRs of HeLa cells did not occur when the arrays were not coupled to Ab's (Figure S9 in the SI).

Micron-sized DNA−biotin−STV−Ab arrays appear capable of binding to and enveloping multiple cells (Figure 5b and Figures S11 and S6h in the SI). Thus, interactions mediated by DNA assemblies as well as DNA hybridization[10] may be used to direct tissue engineering. Large numbers of Ab's would likely be required for efficient bridging of cells. Arrays optimized to uniquely bind multiple surfaces could form the framework for organizing cells on surfaces and 3D matrices, such as the assemblies shown with hydrogels,[30] collagen networks,[31] and patterns using DNA-coated AFM cantilevers.[2] The generic biotin−STV modification allows a variety of biomolecules, such as peptides or aptamers, to be anchored to arrays, which might serve to identify or induce the fate of stem cells.[32] Further, since DNA networks can be systematically varied in size,[26,33,34] it is possible to identify various cells by both the size and color of the fluorescent DNA patches. This could potentially be used for cancer-cell screening. Having many fluorophores positioned very closely to each other on a DNA scaffold enhances the sensitivity to the lower-intensity light used for array detection. It is possible to uniquely color fluorescent multifunctional DNA patches, allowing the location of tethered small molecules, nanoparticles, or other cargo to be identified.

In conclusion, we have illustrated the specific attachment of periodic 2D DNA arrays to cells using two different methods involving biotin−streptavidin and specific antibody−cell surface interactions, as visualized by fluorescence, confocal microscopy, and SEM. A large number of repeating units in a hexagonal DNA array provide an opportunity for loading many copies of identical or different molecules for cellular delivery or interconnection of cells. The assembly strategy is simple and effective, although the preparation of more monodisperse arrays as well as control of the organization, density, and purification of specific biomolecule couplings is required for more complicated applications.

Acknowledgment. We thank the following people for assistance: N. Fera and J. Boucher for cell culture maintenance, M. C. Choi for confocal microscopy, C. Geary for DNA modeling, and M. Schierhorn and M. Cornish for SEM sample preparation and imaging. This work was funded by the Institute for Collaborative Biotechnologies (ICB) through Grant DAAD19-03-D-0004, the U.S. Army Research Office, and Lawrence Livermore National Laboratories through a UCDRD grant. A.Y.K. is grateful for a training grant in molecular virology (T32AI07471). G.B.B. acknowledges a Corning Inc. Foundation Fellowship.

Supporting Information Available: Experimental methods, controls, and additional data. This material is available free of charge via the Internet at http://pubs.acs.org.

References

(1) Stevens, M. M.; George, J. H. *Science* **2005**, *310*, 1135.
(2) Hsiao, S. C.; Crow, A. K.; Lam, W. A.; Bertozzi, C. R.; Fletcher, D. A.; Francis, M. B. *Angew. Chem., Int. Ed.* **2008**, *47*, 8473.
(3) Luo, D.; Saltzman, W. M. *Nat. Biotechnol.* **2000**, *18*, 33.
(4) Rabuka, D.; Forstner, M. B.; Groves, J. T.; Bertozzi, C. R. *J. Am. Chem. Soc.* **2008**, *130*, 5947.
(5) Paulick, M. G.; Bertozzi, C. R. *Biochemistry* **2008**, *47*, 6991.
(6) Chen, X.; Tam, U. C.; Czlapinski, J. L.; Lee, G. S.; Rabuka, D.; Zettl, A.; Bertozzi, C. R. *J. Am. Chem. Soc.* **2006**, *128*, 6292.
(7) Rabuka, D.; Forstner, M. B.; Groves, J. T.; Bertozzi, C. R. *J. Am. Chem. Soc.* **2008**, *130*, 5947.
(8) Kickhoefer, V. A.; Han, M.; Raval-Fernandes, S.; Poderycki, M. J.; Moniz, R. J.; Vaccari, D.; Silvestry, M.; Stewart, P. L.; Kelly, K. A.; Rome, L. H. *ACS Nano* **2009**, *3*, 27.
(9) Swiston, A. J.; Cheng, C.; Um, S. H.; Irvine, D. J.; Cohen, R. E.; Rubner, M. F. *Nano Lett.* **2008**, *8*, 4446.
(10) Gartner, Z. J.; Bertozzi, C. R. *Proc. Natl. Acad. Sci. U.S.A.* **2009**, *106*, 4606.
(11) Rinker, S.; Ke, Y.; Liu, Y.; Chhabra, R.; Yan, H. *Nat. Nanotechnol.* **2008**, *3*, 418.
(12) Williams, B. A.; Lund, K.; Liu, Y.; Yan, H.; Chaput, J. C. *Angew. Chem., Int. Ed.* **2007**, *46*, 3051.
(13) Yan, H.; Park, S. H.; Finkelstein, G.; Reif, J. H.; LaBean, T. H. *Science* **2003**, *301*, 1882.
(14) Park, S. H.; Pistol, C.; Ahn, S. J.; Reif, J. H.; Lebeck, A. R.; Dwyer, C.; LaBean, T. H. *Angew. Chem., Int. Ed.* **2006**, *45*, 735.
(15) He, Y.; Tian, Y.; Ribbe, A. E.; Mao, C. D. *J. Am. Chem. Soc.* **2006**, *128*, 12664.
(16) Li, H. Y.; LaBean, T. H.; Kenan, D. J. *Org. Biomol. Chem.* **2006**, *4*, 3420.
(17) Koyfman, A. Y.; Braun, G.; Magonov, S.; Chworos, A.; Reich, N. O.; Jaeger, L. *J. Am. Chem. Soc.* **2005**, *127*, 11886.
(18) Le, J. D.; Pinto, Y.; Seeman, N. C.; Musier-Forsyth, K.; Taton, T. A.; Kiehl, R. A. *Nano Lett.* **2004**, *4*, 2343.
(19) Lin, C.; Katilius, E.; Liu, Y.; Zhang, J.; Yan, H. *Angew. Chem., Int. Ed.* **2006**, *45*, 5296.
(20) Chhabra, R.; Sharma, J.; Ke, Y.; Liu, Y.; Rinker, S.; Lindsay, S.; Yan, H. *J. Am. Chem. Soc.* **2007**, *129*, 10304.
(21) Lin, C.; Liu, Y.; Yan, H. *Nano Lett.* **2007**, *7*, 507.
(22) Ke, Y.; Lindsay, S.; Chang, Y.; Liu, Y.; Yan, H. *Science* **2008**, *319*, 180.
(23) He, Y.; Chen, Y.; Liu, H.; Ribbe, A. E.; Mao, C. *J. Am. Chem. Soc.* **2005**, *127*, 12202.
(24) He, Y.; Tian, Y.; Chen, Y.; Deng, Z.; Ribbe, A. E.; Mao, C. *Angew. Chem., Int. Ed.* **2005**, *44*, 6694.
(25) He, Y.; Ko, S. H.; Tian, Y.; Ribbe, A. E.; Mao, C. *Small* **2008**, *4*, 1329.
(26) Koyfman, A. Y.; Magonov, S. N.; Reich, N. O. *Langmuir* **2009**, *25*, 1091.
(27) Carpenter, G.; Cohen, S. *Annu. Rev. Biochem.* **1979**, *48*, 193.
(28) Bremer, E.; Samplonius, D. F.; van Genne, L.; Dijkstra, M. H.; Kroesen, B. J.; de Leij, L. F.; Helfrich, W. *J. Biol. Chem.* **2005**, *280*, 10025.
(29) Kawamoto, T.; Sato, J. D.; Le, A.; Polikoff, J.; Sato, G. H.; Mendelsohn, J. *Proc. Natl. Acad. Sci. U.S.A.* **1983**, *80*, 1337.
(30) Ulijn, R. V.; Bibi, N.; Jayawarna, V.; Thornton, P. D.; Todd, S. J.; Mart, R. J.; Smith, A. M.; Gough, J. E. *Mater. Today* **2007**, *10*, 40.
(31) Rhee, S.; Grinnell, F. *Adv. Drug Delivery Rev.* **2007**, *59*, 1299.
(32) Ding, S.; Wu, T. Y.; Brinker, A.; Peters, E. C.; Hur, W.; Gray, N. S.; Schultz, P. G. *Proc. Natl. Acad. Sci. U.S.A.* **2003**, *100*, 7632.
(33) Rothemund, P. W. K. *Nature* **2009**, *440*, 297.
(34) Douglas, S. M.; Dietz, H.; Liedl, T.; Hogberg, B.; Graf, F.; Shih, W. M. *Nature* **2009**, *459*, 414.

JA9015638